



# Formulation development of itraconazole PEGylated nano-lipid carriers for pulmonary aspergillosis using hot-melt extrusion technology

Gauri Shadambikar<sup>a</sup>, Sushrut Marathe<sup>a</sup>, Nan Ji<sup>a</sup>, Mashan Almutairi<sup>a,c</sup>, Suresh Bandari<sup>a</sup>, Feng Zhang<sup>d</sup>, Mahavir Chougule<sup>a</sup>, Michael Repka<sup>a,b,\*</sup>

<sup>a</sup> Department of Pharmaceutics and Drug Delivery, University of Mississippi, University, MS 38677, USA

<sup>b</sup> Pii Center for Pharmaceutical Technology, University of Mississippi, University, MS 38677, USA

<sup>c</sup> Department of Pharmaceutics, College of Pharmacy, University of Hail, Hail 81442, Saudi Arabia

<sup>d</sup> College of Pharmacy, The University of Texas at Austin, TX 78712, USA

## ARTICLE INFO

### Keywords:

Itraconazole  
PEGylation  
Hot-melt extrusion  
Pulmonary drug delivery  
Inhalation  
Nanostructured lipid carriers

## ABSTRACT

Pulmonary delivery is a promising alternative for the oral treatment of pulmonary aspergillosis. This study aimed to develop continuous and scalable itraconazole PEGylated nano-lipid carriers (ITZ-PEG-NLC) for inhalation delivery. The feasibility of preparing NLCs utilizing hot-melt extrusion (HME) coupled with probe sonication was investigated. The process parameters for HME and sonication were varied to optimize the formulation. ITZ-PEG-NLC (particle size,  $101.20 \pm 1.69$  nm; polydispersity index,  $0.26 \pm 0.01$ ) was successfully formulated. The drug entrapment efficiency of ITZ-PEG-NLC was  $97.28 \pm 0.50\%$ . Transmission electron microscopy was used to characterize the shape of the particles. The developed formulations were evaluated for their aerodynamic properties for pulmonary delivery. The lung deposition of ITZ-PEG-NLC was determined using an Anderson Cascade Impactor and Philips Respironics Sami the Seal Nebulizer Compressor. *In vitro* cytotoxicity studies were performed using A549 cells. A burst-release pattern was observed in ITZ-PEG-NLC with a drug release of  $41.74 \pm 1.49\%$  in 60 min. The *in vitro* aerosolization of the ITZ-PEG-NLC formulation showed a mass median aerodynamic diameter of  $3.51 \pm 0.28$   $\mu\text{m}$  and a geometric standard deviation of  $2.44 \pm 0.49$ . These findings indicate that HME technology could be used for the production of continuous scalable ITZ-PEG-NLC.

## 1. Introduction

Inhalation drug delivery is a potential route for the treatment of various pulmonary disorders. It has several advantages compared to the conventional oral or parenteral route. It reduces frequent dosing and avoids first-pass metabolism; further, the inhaled drug directly reaches the lung epithelium, and the process is noninvasive (Lau et al., 2017; Patlolla et al., 2010). In the last few years, there has been a growing interest in the pulmonary route of drug delivery due to the potential use of the lung as a portal for the entry of drugs to the bloodstream, as it has a large surface area for absorption ( $\sim 100$  m<sup>2</sup>) and thin absorption membrane (0.1–0.2  $\mu\text{m}$ ) (Pilcer and Amighi, 2010). The use of biodegradable nanoparticles in inhalation drug delivery has proven to be advantageous as it controls drug release over a prolonged time while protecting the drug from degradation (Patel et al., 2009). Nano-lipid carriers (NLCs) are complex structures that confer higher drug loading

and stability than solid lipid nanoparticles (Puglia et al., 2011). NLCs are surrounded by an outer solid shell, while the inner core is composed of oil that facilitates a higher drug load of lipophilic drugs (Müller et al., 2002).

Pulmonary aspergillosis is an opportunistic fungal disease that occurs in immunocompromised patients (Kousha et al., 2011). Even with the development of new diagnoses and therapies, the overall mortality rate remains approximately 50% (Hope, 2009). It has already been proven that nebulization of antifungal drugs to the lungs enhances therapy by achieving high, localized concentration while avoiding systemic toxicity when compared with the oral route of administration (Alvarez et al., 2007).

Itraconazole (ITZ) is a poorly water-soluble, BCS class II, an anti-fungal drug widely used to treat various fungal infections such as aspergillosis (Maertens and Boogaerts, 2005). It has an n-octanol/water partition coefficient of 5.66 at pH 8.1 (Pardeike et al., 2011). It is known

\* Corresponding author at: Department of Pharmaceutics and Drug Delivery, Pii Center for Pharmaceutical Technology, School of Pharmacy, University of Mississippi, University, MS 38677, USA.

E-mail address: [marepka@olemiss.edu](mailto:marepka@olemiss.edu) (M. Repka).

<https://doi.org/10.1016/j.ijpx.2021.100074>

Received 26 February 2021; Accepted 27 February 2021

Available online 3 March 2021

2590-1567/© 2021 The Author(s).

Published by Elsevier B.V. This is an open access article under the CC BY-NC-ND license

(<http://creativecommons.org/licenses/by-nc-nd/4.0/>).

to cause hepatotoxicity, cardiac dysrhythmia, peripheral neuropathy, and hearing loss, and hence, has limited use in systemic administration (Akkar and Müller, 2003). The inhalation delivery of ITZ at a lower dose overcomes limitations associated with oral delivery.

During the disease state, the pulmonary airways are covered with a layer of particularly viscoelastic mucus that is difficult to penetrate (Schuster et al., 2013; Suk et al., 2016). Mucus clearance and macrophages are the 2 main mechanisms responsible for clearance in the lungs. PEG is a hydrophilic, nonionic, and nontoxic polymer (Lai et al., 2009). The PEGylation of nanoparticles provides a multi-fold benefit. It forms a hydrophilic corona on the nanoparticles that prevents macrophage uptake (phagocytosis) and opsonization (Suk et al., 2016). PEG is an effective steric stabilizer due to its hydrophilicity, charge neutrality, and chain flexibility (Palacio et al., 2016). The formation of the hydrophilic shell is beneficial for penetrating the mucus barrier, shielding particles from aggregation, and providing nanoparticles with salt and serum stability (Forier et al., 2013; Suk et al., 2016, 2009). This multifunctional attribute of PEGylation of the nanoparticles increases lung residence time.

High-pressure homogenization (HPH), micro emulsification, and solvent displacement are some of the current methods used in the preparation of NLCs (Pardeike et al., 2009). However, these methods involve multistep processing including the melting of lipids, dispersion of drug in the molten lipids, the addition of aqueous phase, mixing, and size reduction, making it a batch process (Patil et al., 2015). Solvent displacement has a disadvantage of using organic solvents that need to be removed since even solvent traces could cause toxicity. HPH method is scalable and is the preferred method for the preparation of nanoparticles (Shegokar et al., 2011). However, the method involves a long processing time and batch-to-batch variations (Bhagurkar et al., 2017). A continuous process is always preferred over a batch process in pharmaceutical manufacturing as it reduces the cost of production, labor, and resources. Batch methods pose a risk of batch-to-batch variations and variable product outcomes of the NLCs such as particle size, polydispersity, and drug entrapment efficiency. A continuous process can provide higher efficiency and improved product quality (Patil et al., 2014).

Hot-melt extrusion (HME) technology is a continuous process of pumping raw materials at high temperatures and pressures to obtain a uniform product (Shadambikar et al., 2021; Tiwari et al., 2016). This process offers many advantages over conventional pharmaceutical manufacturing processes. Because it eliminates the use of solvents, it provides environmental advantages along with shorter and efficient processing time to produce the final product (Repka et al., 2007; Zhang et al., 2020). Hence, HME has emerged as an innovative technology to produce pharmaceutical dosage forms such as tablets, capsules, implants, and films over traditional techniques (Kallakunta et al., 2019; Repka et al., 2008; Shadambikar et al., 2020).

The novelty of this study is to investigate the feasibility of the HME technology in the preparation of the inhalable PEGylated itraconazole loaded NLCs (ITZ-PEG-NLC) of <200 nm and to optimize the process to obtain a good quality product. In this study, repeated measures two-way ANOVA was used to understand the effect of process parameters on the physical characteristics and stability of the NLCs. Furthermore, ITZ-PEG-NLC was investigated for the inhalation drug delivery of itraconazole by examining the effects of ITZ-PEG-NLC on the release of itraconazole, aerodynamic properties, and *in vitro* cytotoxicity against A549 cells.

## 2. Materials and methods

### 2.1. Materials

Itraconazole was obtained from TCI Chemicals (Portland, OR), and N-(carbonyl-methoxypolyethyleneglycol-2000)-1,2-distearoyl-sn-glycero-3-phosphoethanolamine sodium salt (mPEG-2K-DSPE sodium salt) was purchased from Lipoid (Ludwigshafen, Germany). Precirol ATO 5

was a generous gift from Gattefossé (Paramus, NJ). Polysorbate 80 and oleic acid were purchased from Acros Organics (Morris, NJ).

### 2.2. Methods

Lipids were selected based on the literature data for the solubility of ITZ. It showed good solubility in solid lipid Precirol ATO 5 and liquid lipid oleic acid (Pardeike et al., 2011). Polysorbate 80 was selected as a surfactant because of its good emulsification and stabilizing properties (Darji et al., 2018). The drug concentration of ITZ was found to be a critical parameter in the stability of NLCs because of its inherently low solubility in lipids. Higher concentrations of ITZ induced precipitation during the preparation of formulations. The process parameters such as the screw speed and screw configuration of the HME and sonication time were considered to affect the formulation characteristics.

#### 2.2.1. Differential scanning calorimetry (DSC)

A differential scanning calorimeter (DSC 25, TA instruments, New Castle, DS, USA) was employed to observe the melting and the recrystallization behavior of the drug with the excipients and to determine the barrel temperature for the hot-melt extruder. Approximately 5 mg of the samples, individually sealed in the aluminum pans were placed over the sample platform. The samples included ITZ, precirol ATO 5, PEG-2K-DSPE and the physical mixture. The reference pan, empty sealed aluminum pan was placed on the reference platform. The pans were heated from 25 to 200 °C at the rate of 10 °C/min under nitrogen purge (50 mL/min).

#### 2.2.2. Preparation of ITZ-PEG-NLC formulation

The preparation involved 2 steps. The first step was to prepare the formulation by pumping all the raw materials into the barrel, and the second step was sonication to obtain particulate NLC. The volumetric feeder and peristaltic pumps were calibrated depending on the ratio of solid physical mixture to liquid lipid and aqueous solution. The composition of the formulation was kept constant for all NLCs (Table 1). A schematic illustration of the ITZ-PEG-NLC formulation by the HME-Probe Sonication system is shown in Fig. 1. Hot-melt extruder (11 mm Process 11, Thermo Fisher Scientific, Karlsruhe, Germany) with a modified screw configuration (Fig. 2) was utilized. The modified screw configuration provided efficient mixing of the solid mixture with the liquid lipid and the aqueous solution. All the materials were exposed to efficient mixing before the ejection of the pre-emulsion.

The drug was uniformly mixed with Precirol ATO 5 and PEG-2K-DSPE using a V-shell blender (Maxblend®, GlobePharma, New Brunswick, NJ, USA) and introduced into the barrel using a volumetric feeder. Oleic acid and aqueous solutions at the temperature equivalent to the extrusion temperature were added into the barrel using a peristaltic pump in zones 2 and 4, respectively. The aqueous solution was introduced into the lipid mixture in zone 4 of the extruder. The barrel temperature for zones 1 and 2 was 120 °C, and the remaining zones had a temperature of 85 °C. Three screw speeds of 50, 100, and 150 rpm were investigated to determine their influence on the product. The resulting hot pre-emulsion was then probe sonicated (Vibra-cell; Sonics and Materials, Inc., Newton, CT) with an amplitude of 40% for size reduction. The sonication time was varied from 5 to 15 min to check the effect of

**Table 1**  
Composition of ITZ-PEG-NLC formulation.

Material	Amount (%w/v)
Itraconazole	0.025
Precirol ATO 5	5.4
Oleic acid	0.6
PEG-2 K-DSPE	1.0
Polysorbate 80	2.0
Water	QS 100 mL

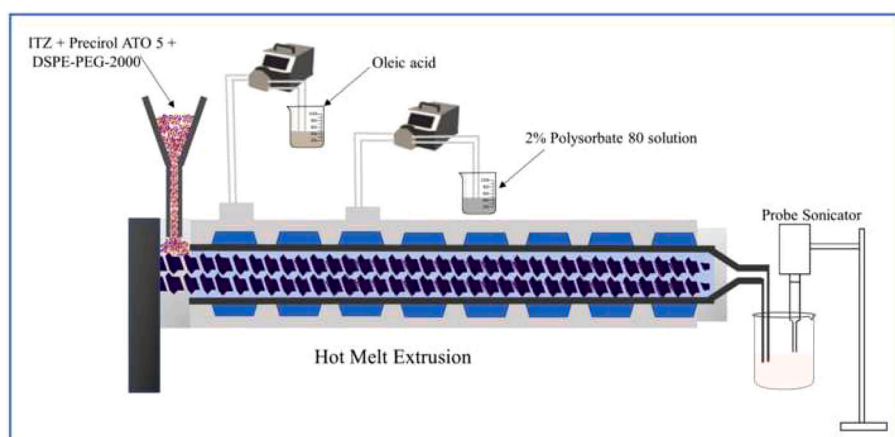


Fig. 1. Schematic illustration of ITZ-PEG-NLC formulation using hot melt extrusion technology and probe sonication.

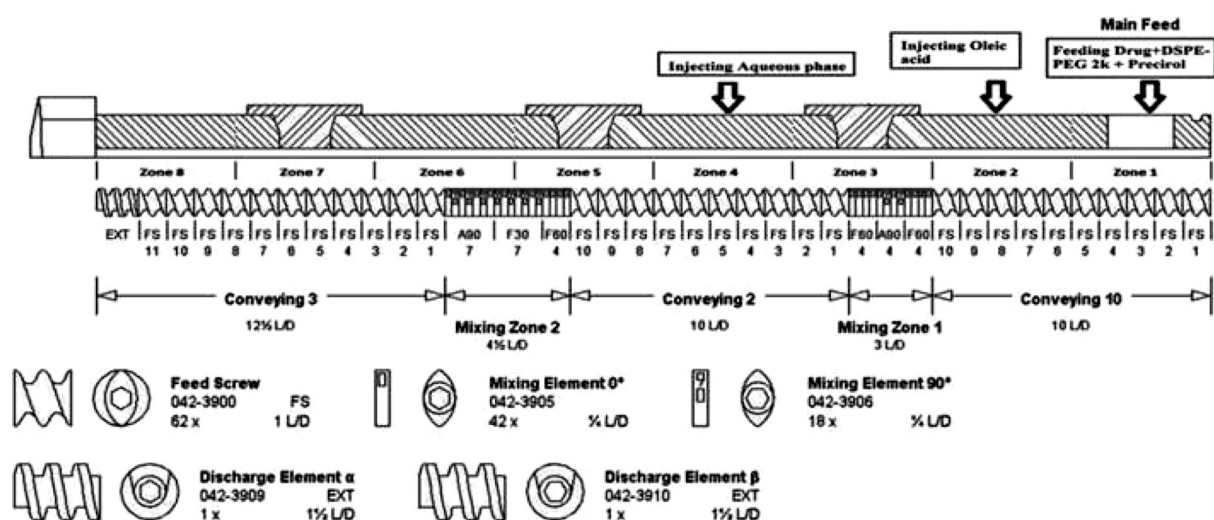


Fig. 2. Modified screw configuration utilized for the preparation of ITZ-PEG-NLC with hot-melt extrusion technology.

sonication time on the ITZ-PEG-NLC particle size. The formulations were stored at 25 °C for 30 days for further characterization.

### 2.3. Characterization of the ITZ-PEG-NLC

#### 2.3.1. Particle size, polydispersity index (PDI), and zeta potential analysis

The particle size, PDI, and zeta potential of the ITZ-PEG-NLC formulations were determined by photon correlation spectroscopy using a Zetasizer Nano ZS Zen3600 (Malvern® Instruments, Malvern, UK) at a temperature of 25 °C and with 173° backscatter detection in disposable folded capillary clear cells. The measurements were obtained using a helium-neon laser, and the particle size data were evaluated based on the volume distribution. Briefly, 10 µL of the sample was diluted to 1000 µL using deionized water, and the particle size and PDI were measured.

#### 2.3.2. HPLC method

Quantification of itraconazole was performed using a Waters HPLC system with a Waters 2489 UV detector utilizing a Luna C18, 250 × 4.6 mm (5 µ) Phenomenex column. The stock solution was prepared in a mixture of DCM:DMSO at a ratio of 4:1 (Pardeike et al., 2016). The mobile phase was composed of a mixture of acetonitrile and 0.1% aqueous solution of glacial acetic acid in a ratio of 80:20. The UV spectrum was recorded at 267 nm with a flow rate of 1 mL/min and an injection volume of 20 µL.

#### 2.3.3. Entrapment efficiency

The entrapment efficiency was determined by calculating the entrapped drug after removal of unentrapped drug using an Amicon® centrifugal filter (MWCO 10 kDa) units centrifuged at 13,000 rpm for 15 min. The filtrate was analyzed using HPLC. The following formula was used to calculate the % entrapment efficiency (EE):

$$\%EE = \frac{\text{Amount of ITZ added} - \text{Amount of ITZ in filtrate}}{\text{Amount of ITZ added}} \times 100$$

#### 2.3.4. Assay (ITZ content)

An accurately measured amount of ITZ-PEG-NLC (50 µL) was added to a 5 mL volumetric flask with the addition of 200 µL of dichloromethane (DCM) and dimethylsulfoxide (DMSO) in a ratio of 4:1, and the volume was made up to the mark with acetonitrile. The sample was centrifuged at 13000 rpm for 15 min and the supernatant was analyzed by HPLC.

#### 2.3.5. Powder X-Ray diffraction analysis

A qualitative powder X-ray diffraction (PXRD) was done (performed at the University of Texas, Austin) to examine the physical state of ITZ in the formulated ITZ-PEG-NLC. The X-ray powder diffraction patterns of the samples were recorded with the Rigaku X-ray system (D/MAX-2500PC, Rigaku Corp., Tokyo, Japan) using Cu rays ( $\lambda = 1.54056 \text{ \AA}$ ) with a voltage of 40 kV and a current of 40 mA, over a 2θ scanning range

of 5°–50°, with a step width of 0.02°/s and a scan speed of 0.02 s.

### 2.3.6. *In vitro* release study

The *in vitro* release studies were conducted on day 0 and day 30 with 10 mL of an aqueous solution containing 20% (w/v) 2-hydroxypropyl-beta cyclodextrin as a dissolution medium in scintillation glass vials. A separate scintillation glass vial with medium and formulation was utilized for each time point. To the medium of each scintillation glass vial, 1 mL of the ITZ-PEG-NLC formulation was added. For every time point, 400 µL of the sample was collected from the respective scintillation glass vial. The sample was centrifuged using a 10 kDa Amicon® filter for 15 min at 13,000 rpm and the permeant was analyzed by HPLC for ITZ released into the medium. The experiments were performed in triplicate. The *in vitro* release method was adopted and modified as reported by (Pardeike et al., 2011). To compare the release profiles of the initial and stability sample, a similarity factor ( $f_2$ ) was calculated. The equation of the similarity factor is represented in the equation below-

$$f_2 = 50 \times \log \left\{ \left[ 1 + \left( \frac{1}{n} \right) \sum_{t=1}^n (R_t - T_t)^2 \right]^{-0.5} \times 100 \right\}$$

where  $R_t$  and  $T_t$  are % dissolved for the initial sample and stability sample, respectively at each time point while  $n$  denotes the number of time points. If the  $f_2$  value of the two release profiles is between 50 and 100, the initial and stable samples are considered similar (Stevens et al., 2015).

### 2.3.7. Viscosity

The viscosity of ITZ-PEG-NLC was measured using a Brookfield cone and plate viscometer (LV-DV-II+ Pro Viscometer, Middleboro, MA, USA). A sample equivalent to 1 mL of the formulation was placed in the cup plate after adjusting the gap between the cone and plate. The formulation in the cup was maintained at 25 °C using a circulating water bath. A CPE 44 spindle was operated at varying speeds from 1 to 50 rpm and the viscosity was recorded using Rheocalc software.

### 2.3.8. Nebulization of the ITZ-PEG-NLC

To observe the effect of nebulization on particle size and PDI, the ITZ-PEG-NLC was nebulized using a Philips Respironics Sami the Seal Nebulizer Compressor. The particle size and PDI of the formulation before and after nebulization were measured ( $n = 3$ ).

### 2.3.9. *In vitro* aerosol characterization

The aerodynamic particle size distribution was measured using an 8 stage non-viable Anderson cascade impactor (ACI) (Westech® Scientific Instruments, UK). To ensure an efficient particle capture during nebulization, each plate on the impactor was coated with polysorbate 80. The ITZ-PEG-NLC formulation was nebulized for 10 min into the cascade impactor operated at a flow rate of 28.3 L/min. After nebulization with the Philips Respironics Sami the Seal Nebulizer Compressor, the formulations deposited on the impactor stages (0–7) and the filter were collected, and the amount of itraconazole was analyzed using HPLC. The formulations were tested in triplicate, and the mass median aerodynamic diameter (MMAD), geometric standard deviation (GSD) and fine particle fraction (FPF) were calculated.

### 2.3.10. *In vitro* cell viability

The cytotoxicity of ITZ-PEG-NLC was evaluated in a human adenocarcinoma alveolar basal epithelial A549 cell line. For comparison, a PEG-placebo was prepared for the cell viability studies. The A549 cells were seeded in 96-well microtiter plates at a density of 5000 cells/well and after overnight incubation, the cells were treated with various concentrations of PEG-Placebo and ITZ-PEG-NLC diluted in the cell growth medium. The cells were cultured in HyClone™ Dulbecco's modified Eagle medium and maintained at 37 °C with 5% CO<sub>2</sub> in a

humidified incubator. The cells were incubated for 24, 48, and 72 h. The cell viability was determined for each treatment at regular time intervals using a crystal violet assay. The relative cell number was calculated as the ratio of the absorbance of the treated well to that of the untreated control. The obtained results were analyzed by one-way ANOVA.

### 2.3.11. Morphological characteristics using Tandem electron microscopy

A 20 µL drop of the sample was placed on a sheet of clean parafilm. A freshly glow-discharged 200 mesh copper grids coated with thin carbon film was floated film-side down on the drop of sample. After 30 s, the grid was removed from the drop and the excess sample was removed by touching a piece of filter paper to the edge of the grid. Before complete drying, the grids were placed on a sample size down on a drop of ultrapure water and immediately removed. Excess water was removed, and the grid sample side down was placed on a drop of 1% uranyl acetate. Images were generated on a JEOL JEM-1400 Flash TEM and captured on a Gatan One View digital camera (studies performed at the University of Tennessee, Knoxville).

### 2.3.12. Statistical analysis

Statistical analysis was conducted using one-way ANOVA and two-way repeated measures ANOVA (JASP 0.13.1.0). Sample differences were deemed statistically significant if  $p < 0.05$ .

## 3. Results and discussion

### 3.1. Preparation of ITZ-PEG-NLC

Process parameters such as the screw speed of HME and the sonication time were optimized for the formulation of ITZ-PEG-NLC. The screw design, zone of liquid addition, drug and lipid concentration for the ITZ-PEG-NLC were optimized from the preliminary trials. The preliminary trials indicated that a modified screw design, with a mixing element after zone 1 and 2, was efficient in mixing of oil with the solid lipid and itraconazole. Further, the next mixing element after addition of the aqueous phase provided efficient mixing of all of the components in the barrel before ejection of the product from the barrel. The zone of liquid addition for the aqueous solution was determined based on the screw configuration and was optimized to be zone 4 compared to zone 3. The barrel temperature for all of the zones was optimized based on the thermal analysis of the physical mixture. The zone 1 temperature was higher than the rest of the barrel to facilitate efficient melting and mixing of itraconazole within the components. In NLC preparation, the formation of the pre-emulsion is of utmost importance to achieve a stable formulation. The sonication time of the hot pre-emulsion influenced the size reduction and stability of the formulation. For all the HME runs, the feeding rate and torque were controlled to prevent formulation variations. The torque value obtained was less than 5% for all runs.

### 3.2. Differential scanning calorimetry

Differential Scanning Calorimetry was used for analyzing the melting and recrystallization behavior of the drug within the lipid phase and is shown in Fig. 3. The melting point of ITZ is reported to be between 166 and 170 °C (USP Monograph [WWW Document], 2021). A melting endothermic depression can be spotted at ~169 °C. The physical mixture of the drug in the lipid phase indicates a melting peak of the lipids at ~70 °C, coinciding with the melting point of Precirol ATO 5. The drug-lipid mixture thermograms did not show any endothermic peak for ITZ, suggesting either complete solubility of the drug in the lipid phase or conversion of the drug from crystalline to amorphous form.

### 3.3. Particle size, PDI, and zeta potential analysis

The particle size is an important parameter for the pulmonary drug

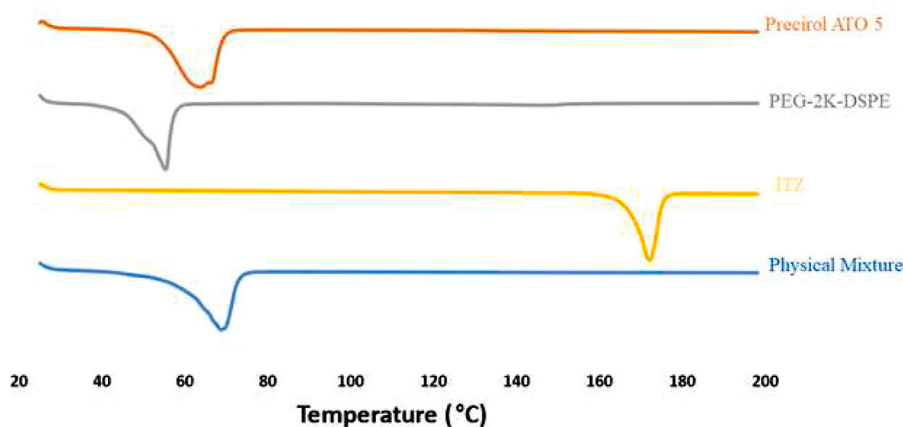


Fig. 3. Differential Scanning Calorimetry thermograms.

delivery. To achieve enhanced delivery of the drug, the particle size of the NLCs needs to be smaller, thus accommodating a larger number of nanoparticles into the micron-sized droplets. As well as the high specific surface area of the NLCs provides high contact surface with the lung tissue (Rivolta et al., 2011; Yang et al., 2008). Table 2 presents the particle size, PDI, and zeta potential of the 9 formulations on day 0 and day 30.

NLC formulations need to be stable on storage otherwise the particle size and PDI of a freshly prepared formulation and its physicochemical characteristics may change over time. Hence, a two-way repeated measures ANOVA was conducted on particle size, PDI, and zeta potential of the ITZ-PEG-NLC to evaluate the effects of the screw speed (*rpm*) and sonication time (*min*) on storage stability (*stability*). Assumptions of normality and sphericity were met owing to the balanced nature of the design. The within-subject effects in the repeated measures ANOVA describe the effects of the independent variables on the same sample measured at different time points (Table 3). These effects are seen as an interaction of the independent variables with the time-dependent variable, in this case, storage stability (*stability*). Therefore, in the analysis, the effect of the screw speed (*rpm*) and the sonication time (*min*) on the particle size, PDI, and zeta potential on storage is described as the interaction between storage *stability* and screw speed (*stability\*rpm*), storage *stability* and sonication time (*stability\*min*), and storage *stability*, screw speed, and sonication time (*stability\*rpm\*min*). The between-

Table 3

Within-subject effects of the independent variables.

	Particle size <i>p</i> -value	PDI <i>p</i> -value	Zeta potential <i>p</i> -value
Stability	0.011	0.902	<0.001
Stability* <i>rpm</i>	0.001	<0.001	0.818
Stability* <i>min</i>	<0.001	<0.001	0.055
Stability* <i>rpm*min</i>	0.269	<0.001	0.135

subject effects explain the influence of process variables (screw speed and sonication time) on different samples at different levels of independent variables (Table 4). They can be used to understand the direct effect of screw speed and *rpm* on particle size, PDI, and zeta potential of

Table 4

Between-subject effects of the independent variables.

	Particle size <i>p</i> -value	PDI <i>p</i> -value	Zeta potential <i>p</i> -value
<i>Rpm</i>	<0.001	0.040	0.941
<i>Mins</i>	<0.001	0.011	0.002
<i>Rpm*mins</i>	<0.001	0.132	0.734

Table 2

Particle Size, PDI, and Zeta Potential of NLC Formulations for Day 0 and Day 30.

Formulation No.	Screw speed (rpm)	Sonication time (minutes)	Day 0			Day 30		
			Particle size (nm)	PDI	Zeta potential (mV)	Particle size (nm)	PDI	Zeta potential (mV)
F 1	50	5	172.7 ± 14.66	0.24 ± 0.03	-24.8 ± 5.49	178.6 ± 10.04	0.39 ± 0.04	-21.6 ± 0.45
F 2	50	10	101.2 ± 1.69	0.26 ± 0.01	-19.1 ± 5.84	99.61 ± 1.33	0.22 ± 0.03	-15.6 ± 2.22
F 3	50	15	79.11 ± 1.66	0.20 ± 0.04	-23.6 ± 3.76	142.9 ± 6.75	0.37 ± 0.07	-16.8 ± 0.52
F 4	100	5	114.9 ± 4.09	0.34 ± 0.06	-26.3 ± 1.19	200.4 ± 6.24	0.05 ± 0.03	-18.6 ± 0.17
F 5	100	10	84.95 ± 1.19	0.22 ± 0.02	-20.2 ± 2.29	134.8 ± 0.36	0.17 ± 0.03	-16.8 ± 0.57
F 6	100	15	87.54 ± 1.60	0.24 ± 0.03	-22.5 ± 6.34	168.5 ± 9.2	0.38 ± 0.09	-17.4 ± 1.35
F 7	150	5	99.92 ± 0.89	0.22 ± 0.05	-28.9 ± 4.56	185.9 ± 29.06	0.22 ± 0.06	-19.20 ± 1.52
F 8	150	10	103.8 ± 2.72	0.281 ± 0.02	-20.3 ± 1.69	193 ± 3.08	0.22 ± 0.06	-18.2 ± 0.55
F 9	150	15	107.6 ± 1.79	0.372 ± 0.06	-20.5 ± 1.14	207.9 ± 7.17	0.27 ± 0.03	-16.7 ± 0.5

nanoparticles.

The within-subject interactions of the *stability\*rpm* and *stability\*mins* on the particle size analysis were significant ( $p < 0.001$ ) indicating a significant difference between particle size measured on day 1 and day 30 of the formulations prepared with different screw speeds and sonication times (Fig. 4a). For the PDI, the *stability\*rpm\*min* interaction was significant ( $p < 0.001$ ) indicating a significant effect of screw speed, sonication time, and storage stability together on the difference between the PDI on day 1 and day 30 of the same formulation (Fig. 4b). In case of zeta potential, only the storage (*stability*) had a significant effect ( $p < 0.001$ ), while the screw speed (*rpm*) and sonication time (*mins*) did not have a significant effect on the difference in zeta potential observed for the formulations on Day 1 and same formulations measured on day 30 (Fig. 4c).

From the between-subject effects, it was observed that particle size was significantly affected by the screw speed and sonication time, evidenced by a significant effect on the particle size of the *rpm\*min* interaction ( $p < 0.001$ ). The *rpm\*min* did not have a significant effect on the particle size ( $p = 0.132$ ), but *rpm* ( $p = 0.040$ ) and *mins* ( $p = 0.011$ ) independently had a significant effect on PDI. For zeta potential, only *mins* ( $p < 0.002$ ) had a significant effect, while *rpm* ( $p = 0.941$ ) and *rpm\*min* interaction ( $p = 0.734$ ) did not show any significant effect.

The increase in particle size on storage observed for screw speeds of 100 rpm and 150 rpm is likely attributed to the decrease in residence time of the materials inside the barrel that limited the mixing of aqueous and lipid phases for the pre-emulsion. For probe sonication, a decrease in particle size of the formulation was observed with increasing time. It is known that particles of smaller size have higher surface free energy and need higher concentrations of stabilizers (Phan and Haes, 2019). For the sonication time of 15 min on day 0, small particle size was observed, but the formulation was unstable. As the formulation cooled over a longer sonication time, the NLCs started to solidify and the continuous energy input from the sonication probe fractured these solidifying nanoparticles. These incompletely solidified NLCs started to agglomerate and sediment on storage.

Post-hoc analysis was performed to understand the main effects of the independent variables as well as the interactions. The formulation NLC-2 (screw speed 50 rpm and sonication time 10 min) was selected for further evaluation as it showed the smallest particle size and no significant change in particle size, PDI, and zeta potential on storage for 30

days.

### 3.4. Entrapment efficiency and assay

The entrapment efficiency of all formulations investigated was between 95% and 98%. The percent entrapment efficiency of the ITZ-PEG-NLC obtained for formulation NLC-2 was  $97.28 \pm 0.50\%$ . The obtained assay (drug content) for all formulations was more than 95%. The assay of the NLC-2 formulation was found to be  $96.40 \pm 4.06\%$ .

### 3.5. Powder X-Ray diffraction analysis

The Fig. 5 represents the PXRD stacked plots for the ITZ, ITZ-PEG-NLC and the placebo-PEG-NLC. The sharp PXRD peaks for ITZ indicated crystalline nature. The PXRD plots revealed the absence of characteristic ITZ peaks at  $2\theta$  values of 14.50 and between  $17\theta - 19\theta$  in the ITZ-PEG-NLC. The sharp peak intensity at 20.50 of the ITZ was substantially reduced in the ITZ-PEG-NLC. As the drug was completely solubilized in the lipid matrix, the crystallinity of the drug was lost and an homogenous formulation was achieved with the amorphous nature of ITZ in the formulation. This observation is in accordance with reported studies (Lim et al., 2014; Parikh et al., 2016).

### 3.6. In vitro drug release

The release profile of ITZ from the formulation (NLC-2) on day 0 and day 30 is presented in Fig. 6. The drug was released from the PEGylated nanoparticles with an initial burst release of  $41.74 \pm 1.49\%$  in 1 h followed by a slower release for day 0 formulation. Similar results were observed with the initial burst release of  $43.6 \pm 0.5\%$  in 1 h and then a controlled release for the stability formulation on day 30. The similarity factor ( $f_2$ ) value for the day 0 and day 30 formulations was 70.17. The observed burst release could be due to the drug being loosely bound or near the surface. The drug at the center of the nanoparticle core was not released as nanoparticles remained intact and maintained their integrity for the duration of the study. Thus, a plateau in drug release was observed after 24 h as the drug at the surface was released. This is consistent with the hypothesis of intracellular drug delivery; where after the initial burst, the nanoparticles will carry the drug into the cell on cellular uptake (Rivolta et al., 2011). The nanoparticles degrade by

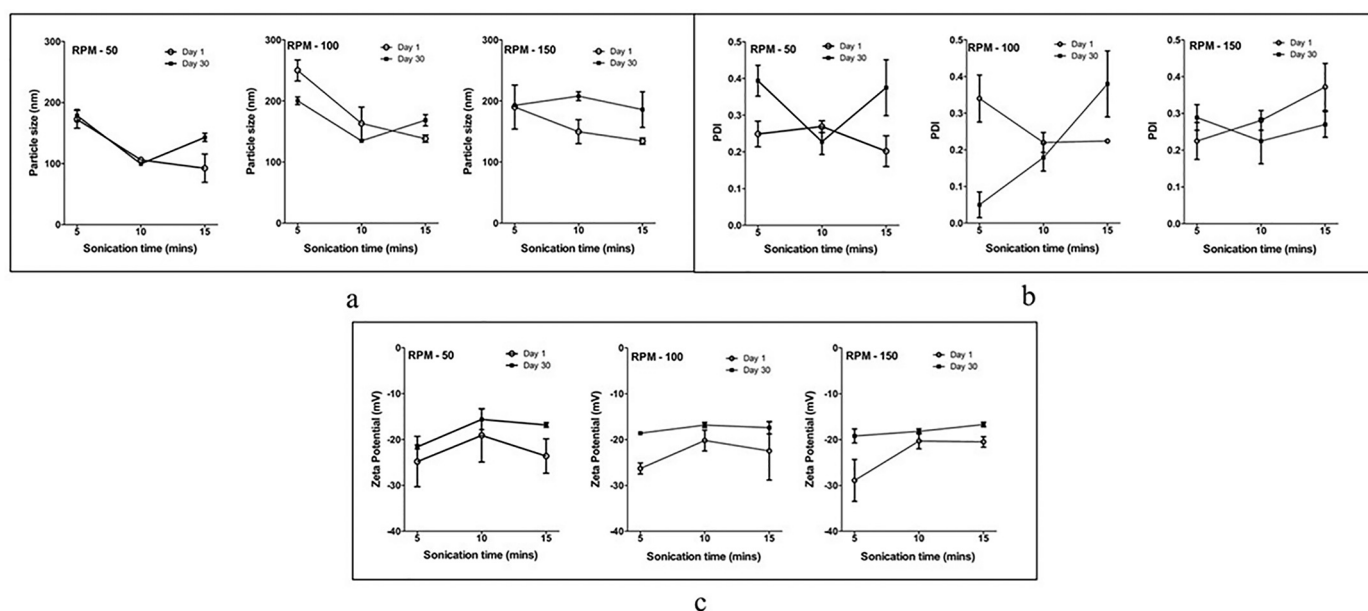


Fig. 4. Effect of parameters on attributes of the formulation. 3a- Effect of parameters on the particle size of formulation. 3b- Effect of parameters on the PDI of the formulation. 3c- Effect of parameters on the zeta potential of the formulation.

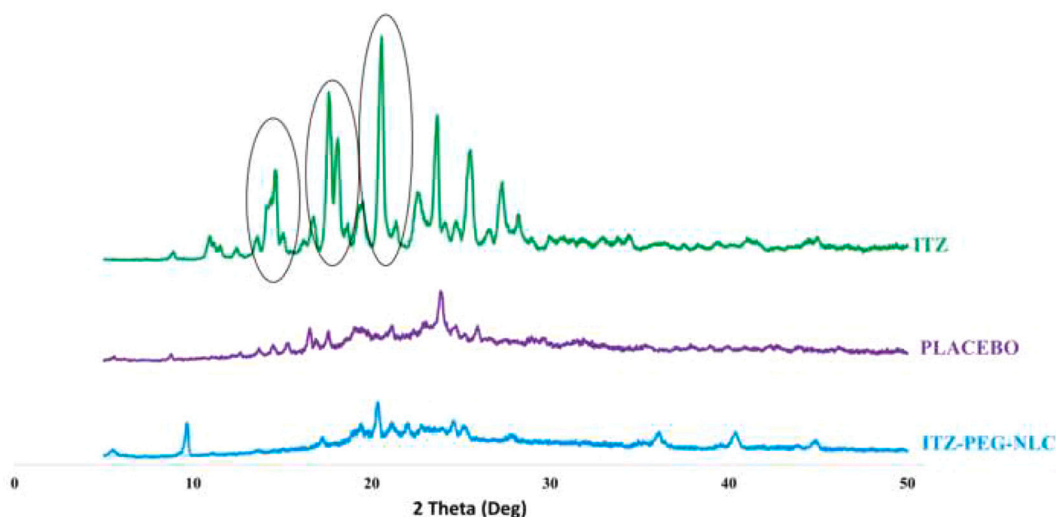


Fig. 5. PXRD Diffractograms of pure ITZ, ITZ-PEG-NLC formulation (F-2) and placebo formulation.

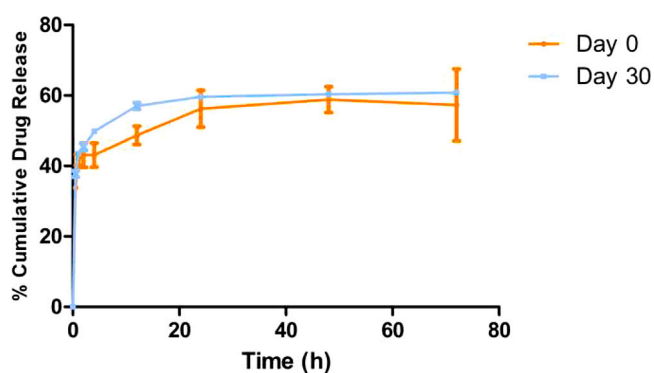


Fig. 6. *In vitro* release of ITZ-PEG-NLC in 10 mL of 20% (w/v) 2-hydroxypropyl-beta cyclodextrin (mean  $\pm$  SD,  $n = 3$ ).

activity of intracellular lipases and release the drug within the cell (Olbrich et al., 2002).

### 3.7. Viscosity

The NLC-2 formulation showed (Fig. 7) a decrease in viscosity with increasing spindle speed. During the nebulization process, high shear is applied to the formulation to form aerosols. It has been shown that the

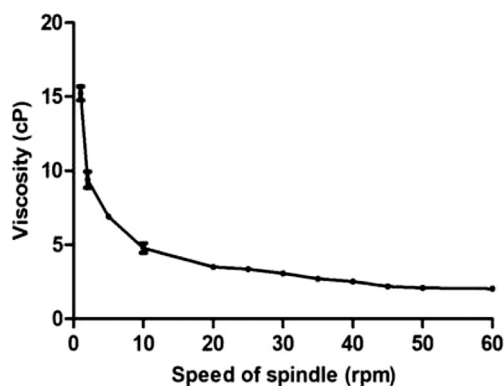


Fig. 7. Viscosity against the speed of spindle (CPE 44) using the Brookfield cone and plate viscometer, (each error bar represents standard deviation,  $n = 3$ ).

viscosity of the formulation plays an important role in determining the droplet size during nebulization (McCallion et al., 1995). Hence, it was necessary to determine the effect of shear on the viscosity of the formulation. The formulation exhibited a non-Newtonian behavior and showed a decreasing trend with the application of higher shear.

### 3.8. Nebulization of the ITZ-PEG-NLC

Before nebulization of the formulation using the Philips Respironics Sami the Seal Nebulizer Compressor, the particle size was  $101.20 \pm 1.69$  nm with a PDI of  $0.26 \pm 0.02$ . The entrapment efficiency observed was  $97.28 \pm 0.50\%$ . After nebulization, the particle size, PDI, and entrapment efficiency were  $103.56 \pm 5.60$ ,  $0.25 \pm 0.04$ , and  $97.14 \pm 0.89\%$ , respectively. This test was carried out to observe the effect of the jet nebulizer on the aerosolization of the formulation. It is known that jet nebulization can disturb the structural integrity of the nanoparticles, agglomerate, or aggregate, thus leading to instability (Dailey et al., 2003). Fig. 8 shows the particle size and PDI of the ITZ-PEG-NLC before and after nebulization using a Philips Respironics Sami the Seal Nebulizer Compressor showing that the formulation was stable and that nebulization did not cause aggregation.

### 3.9. Aerodynamic characterization

The aerodynamic characteristics of the ITZ-PEG-NLC formulation were determined using the ACL; such determination is essential to understand the fate of nanoparticles in the lungs after nebulization. The MMAD of the formulation is an important parameter as it determines the amount of drug deposition in the lung. The droplet size should be in the range of  $1 \mu\text{m}$  to  $5 \mu\text{m}$  for optimal deep lung drug delivery by inhalation. Droplets  $>5 \mu\text{m}$  are deposited in the conducting airways and oropharyngeal region, while droplets  $<1 \mu\text{m}$  can be exhaled (Labiris and Dolovich, 2003a). Particles  $<3 \mu\text{m}$  have an approximately 80% chance of reaching the lower airways with 50–60% being deposited in the alveoli (Labiris and Dolovich, 2003b; Patton, 1996). The results showed an MMAD of  $3.51 \pm 0.28 \mu\text{m}$  and GSD of  $2.44 \pm 0.49$  for the NLC-2 formulation.

The MMAD of our formulation was within the specified inhalable range of less than  $5 \mu\text{m}$ . The variability in the particle diameter within the aerosol was measured by GSD; the result showed that the formulation was a heterodisperse aerosol ( $\text{GSD} > 1.2$ ). This was observed by distribution of the formulation at different stages in the ACL. About  $85.57 \pm 2.98\%$  of the formulation was recovered indicating a good efficiency in dosing from the nebulizer. FPF can be defined as the

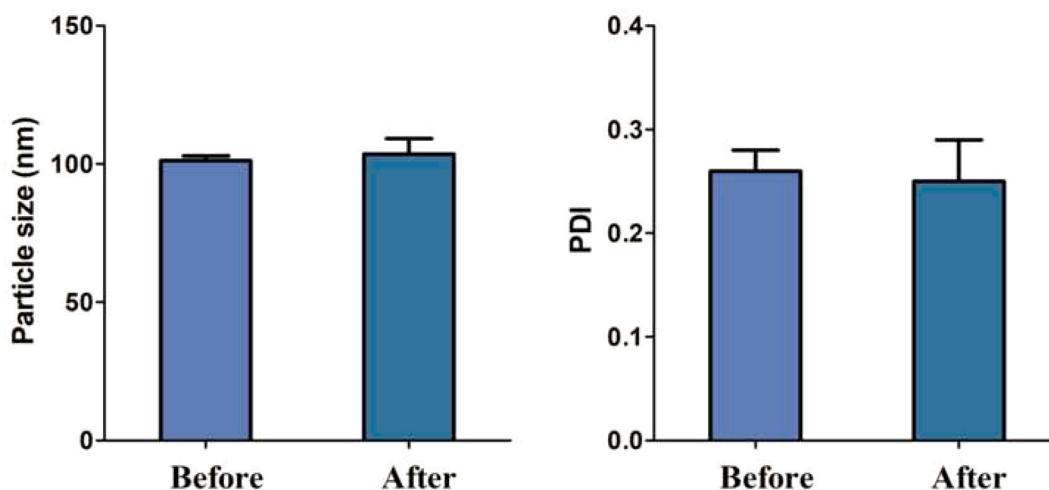


Fig. 8. Particle size and PDI of the ITZ-PEG-NLC before and after nebulization using Philips Respironics Sami the Seal Nebulizer Compressor, (each error bar represents standard deviation,  $n = 3$ ).

percent ratio of amount of drug *i.e.* deposited on the stages having cut-off diameter less than  $4.7 \mu\text{m}$  to the recovery. The results showed an FPF of  $52.23 \pm 7.07\%$ . A higher percent FPF ensures efficient delivery of dose to the lungs as the fine droplets will be able to deliver the drug to the deeper lung tissues. The amount of ITZ deposited over the eight stages of the ACI is summarized in Fig. 9. The results showed that the nanoparticles of the ITZ-PEG-NLC formulation possessed good aerosolization properties and were suitable for deep lung tissue drug delivery.

### 3.10. *In vitro* cell viability

It is important to determine the safety of the formulation when in contact with lung epithelial cells. The cytotoxicity of the ITZ-PEG-NLC and placebo PEG-NLC formulations was determined using A549 cells by incubation at various formulation concentrations for 24, 48, and 72 h (Fig. 10). The cells were treated with ITZ-PEG-NLC and PEG-Placebo diluted 500-, 1000-, and 2000-times ( $0.5 \mu\text{g}/\text{mL}$ ,  $0.25 \mu\text{g}/\text{mL}$ ,  $0.125 \mu\text{g}/\text{mL}$  respectively) to match the *in vivo* dilution on dosing. The treated cells did not show any significant difference ( $p > 0.05$ ) in cell viability

when compared to the untreated cells (control). *In vitro* cell viability results showed no direct relationship between ITZ concentration and exposure time, demonstrating the safety of the formulation. From the obtained results we can say that this formulation can be used for longer duration of treatment as no toxic effects of the formulation were seen on the cells on continuous exposure for up to 48 h.

### 3.11. Tandem electron microscopy

Tandem electron microscopy was performed on the ITZ-PEG-NLC formulation F2 to understand the shape and morphology of the NLCs. As shown in Fig. 11, the nanoparticles were spherical, and the observed particle size paralleled that obtained by the dynamic light scattering.

## 4. Conclusion

Pegylated itraconazole NLC was prepared using HME along with probe sonication. Continuous production of NLCs can be achieved by this method by optimizing the parameters of HME such as screw speed, screw design, and barrel temperature. Utilizing this method minimizes

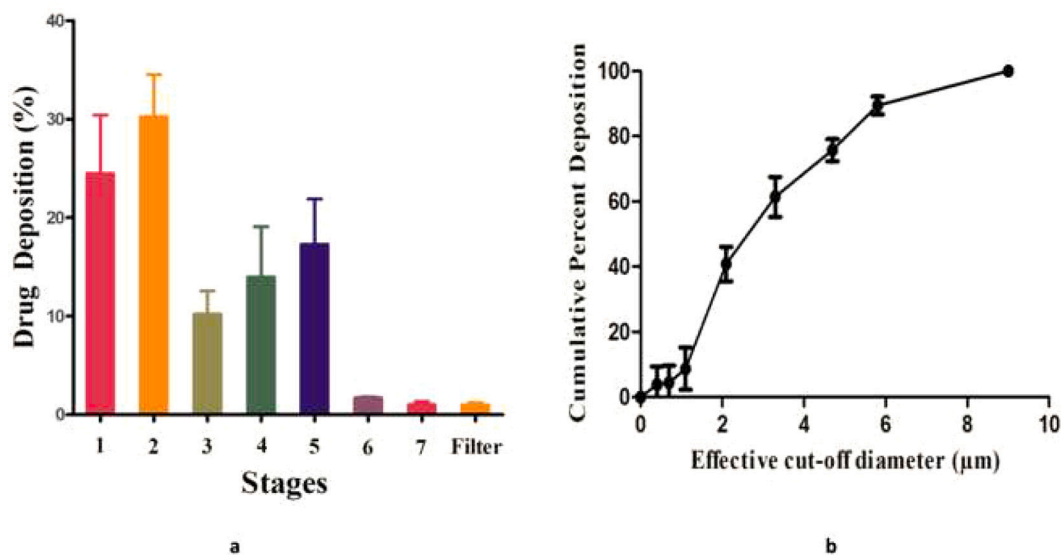


Fig. 9. a-Amount of ITZ deposited on each stage of Anderson cascade impactor using the Philips Respironics Sami the Seal Nebulizer Compressor, b-Cumulative mass deposition versus the Anderson Cascade Impactor effective cut-off diameters, (each error bar represents standard deviation,  $n = 3$ ).

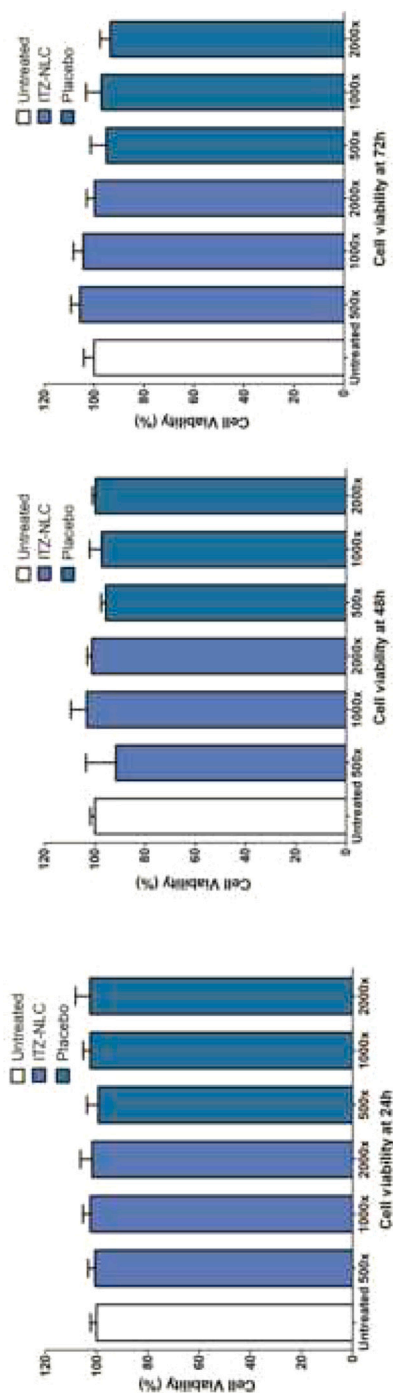


Fig. 10. Cell viability measured by the crystal violet assay for the ITZ-PEG-NLC against A549 cell line. (For interpretation of the references to colour in this figure legend, the reader is referred to the web version of this article.)

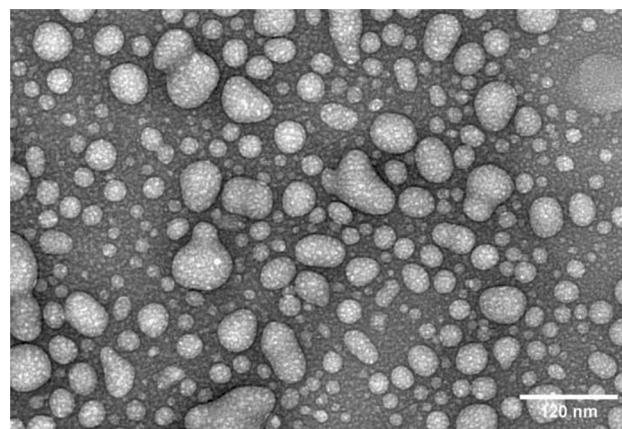


Fig. 11. Tandem Electron Microscopy of ITZ-PEG-NLC formulation F2.

the issues and variations associated with conventional batch methods of nano-formulations production. Our experiments demonstrated that the process parameters influence the formulation quality, with pre-emulsion largely determining the final quality of the formulation. A formulation method for preparing nanoscale particles having high entrapment efficiency and NLCs with good aerosolization properties was developed. The formulation was nebulized without aggregation and agglomeration. The drug formulation was found to be nontoxic to epithelial lung cells. TEM particles showed the spherical nature of the particles. We conclude that the formulation of itraconazole PEGylated nanoparticles prepared by using HME technology may be considered as a potential pulmonary drug delivery system with manufacturing scalability.

#### Author contribution

Research Idea: Gauri Shadambikar, Sushrut Marathe, and Michael Repka; Investigation: Gauri Shadambikar, Sushrut Marathe, Nan Ji, Mashan Almutairi, Feng Zhang; Original Draft Preparation: Gauri Shadambikar; Review and Editing: Suresh Bandari, Mahavir Chougule, Michael Repka.

#### Funding

This project was supported by The University of Mississippi Graduate School Research Grant Award for 2020.

#### Declaration of Competing Interest

The authors declare that they have no known competing financial interests or personal relationships that could have appeared to influence the work reported in this paper.

#### References

- Akkar, A., Müller, R.H., 2003. Intravenous itraconazole emulsions produced by SolEmuls technology. *Eur. J. Pharm. Biopharm.* [https://doi.org/10.1016/S0939-6411\(03\)00063-8](https://doi.org/10.1016/S0939-6411(03)00063-8).
- Alvarez, C.A., Wiederhold, N.P., McConville, J.T., Peters, J.I., Najvar, L.K., Graybill, J.R., Coalson, J.J., Talbert, R.L., Burgess, D.S., Bocanegra, R., Johnston, K.P., Williams, R. O., 2007. Aerosolized nanostructured itraconazole as prophylaxis against invasive pulmonary aspergillosis. *J. Inf. Secur.* <https://doi.org/10.1016/j.jinf.2007.01.014>.
- Bhagurkar, A.M., Repka, M.A., Murthy, S.N., 2017. A novel approach for the development of a nanostructured lipid carrier formulation by hot-melt extrusion technology. *J. Pharm. Sci.* <https://doi.org/10.1016/j.xphs.2016.12.015>.
- Dailey, L.A., Schmehl, T., Gessler, T., Wittmar, M., Grimminger, F., Seeger, W., Kissel, T., 2003. Nebulization of biodegradable nanoparticles: Impact of nebulizer technology and nanoparticle characteristics on aerosol features. *J. Control. Release* 86, 131–144. [https://doi.org/10.1016/S0168-3659\(02\)00370-X](https://doi.org/10.1016/S0168-3659(02)00370-X).
- Darji, M.A., Lalde, R.M., Marathe, S.P., Mulay, T.D., Fatima, T., Alshammari, A., Lee, H. K., Repka, M.A., Narasimha Murthy, S., 2018. Excipient stability in oral solid dosage forms: a review. *AAPS PharmSciTech.* <https://doi.org/10.1208/s12249-017-0864-4>.

- Foier, K., Messiaen, A.S., Raemdonck, K., Deschout, H., Rejman, J., De Baets, F., Nelis, H., De Smedt, S.C., Demeester, J., Coenye, T., Braeckmans, K., 2013. Transport of nanoparticles in cystic fibrosis sputum and bacterial biofilms by single-particle tracking microscopy. *Nanomedicine*. <https://doi.org/10.2217/nnm.12.129>.
- Hope, W.W., 2009. Invasion of the alveolar-capillary barrier by *Aspergillus* spp.: Therapeutic and diagnostic implications for immunocompromised patients with invasive pulmonary aspergillosis. *Med. Mycol.* <https://doi.org/10.1080/13693780802510232>.
- Kallakunta, V.R., Sarabu, S., Bandari, S., Tiwari, R., Patil, H., Repka, M.A., 2019. An update on the contribution of hot-melt extrusion technology to novel drug delivery in the twenty-first century: part I. *Expert Opin. Drug Deliv.* <https://doi.org/10.1080/17425247.2019.1609448>.
- Kousha, M., Tadi, R., Soubani, A.O., 2011. Pulmonary aspergillosis: a clinical review. *Eur. Respir. Rev.* <https://doi.org/10.1183/09059180.00001011>.
- Labiris, N.R., Dolovich, M.B., 2003a. Pulmonary drug delivery. Part I: Physiological factors affecting therapeutic effectiveness of aerosolized medications. *Br. J. Clin. Pharmacol.* <https://doi.org/10.1046/j.1365-2125.2003.01892.x>.
- Labiris, N.R., Dolovich, M.B., 2003b. Pulmonary drug delivery. Part I: Physiological factors affecting therapeutic effectiveness of aerosolized medications. *Br. J. Clin. Pharmacol.* <https://doi.org/10.1046/j.1365-2125.2003.01892.x>.
- Lai, S.K., Wang, Y.Y., Hanes, J., 2009. Mucus-penetrating nanoparticles for drug and gene delivery to mucosal tissues. *Adv. Drug Deliv. Rev.* <https://doi.org/10.1016/j.addr.2008.11.002>.
- Lau, M., Young, P.M., Traini, D., 2017. A review of co-milling techniques for the production of high dose dry powder inhaler formulation. *Drug Dev. Ind. Pharm.* <https://doi.org/10.1080/03639045.2017.1313858>.
- Lim, W.M., Rajinikanth, P.S., Mallikarjun, C., Kang, Y.B., 2014. Formulation and delivery of itraconazole to the brain using a nanolipid carrier system. *Int. J. Nanomedicine*. <https://doi.org/10.2147/IJN.S57565>.
- Maertens, J., Boogaerts, M., 2005. The place for itraconazole in treatment. *J. Antimicrob. Chemother.* <https://doi.org/10.1093/jac/dki222>.
- McCallion, O.N.M., Taylor, K.M.G., Thomas, M., Taylor, A.J., 1995. Nebulization of Fluids of Different Physicochemical Properties with Air-Jet and Ultrasonic Nebulizers. *Pharm. Res. An Off. J. Am. Assoc. Pharm. Sci.* <https://doi.org/10.1023/A:1016205520044>.
- Müller, R.H., Radtke, M., Wissing, S.A., 2002. Nanostructured lipid matrices for improved microencapsulation of drugs. *Int. J. Pharm.* [https://doi.org/10.1016/S0378-5173\(02\)00180-1](https://doi.org/10.1016/S0378-5173(02)00180-1).
- Olbrich, C., Kayser, O., Müller, R.H., 2002. Lipase degradation of Dynasan 114 and 116 solid lipid nanoparticles (SLN) - effect of surfactants, storage time and crystallinity. *Int. J. Pharm.* [https://doi.org/10.1016/S0378-5173\(02\)00035-2](https://doi.org/10.1016/S0378-5173(02)00035-2).
- Palacio, J., Agudelo, N.A., Lopez, B.L., 2016. PEGylation of PLA nanoparticles to improve mucus-penetration and colloidal stability for oral delivery systems. *Curr. Opin. Chem. Eng.* <https://doi.org/10.1016/j.coch.2015.11.006>.
- Pardeike, J., Hommoss, A., Müller, R.H., 2009. Lipid nanoparticles (SLN, NLC) in cosmetic and pharmaceutical dermal products. *Int. J. Pharm.* <https://doi.org/10.1016/j.ijpharm.2008.10.003>.
- Pardeike, J., Weber, S., Haber, T., Wagner, J., Zarfl, H.P., Plank, H., Zimmer, A., 2011. Development of an Itraconazole-loaded nanostructured lipid carrier (NLC) formulation for pulmonary application. *Int. J. Pharm.* <https://doi.org/10.1016/j.ijpharm.2011.07.040>.
- Pardeike, J., Weber, S., Zarfl, H.P., Pagitz, M., Zimmer, A., 2016. Itraconazole-loaded nanostructured lipid carriers (NLC) for pulmonary treatment of aspergillosis in falcons. *Eur. J. Pharm. Biopharm.* <https://doi.org/10.1016/j.ejpb.2016.07.018>.
- Parikh, T., Sandhu, H.K., Talele, T.T., Serajuddin, A.T.M., 2016. Characterization of solid dispersion of itraconazole prepared by solubilization in concentrated aqueous solutions of weak organic acids and drying. *Pharm. Res.* <https://doi.org/10.1007/s11095-016-1890-8>.
- Patel, G., Chougule, M., Singh, M., Misra, A., 2009. Nanoliposomal dry powder formulations. *Methods Enzymol.* [https://doi.org/10.1016/S0076-6879\(09\)64009-X](https://doi.org/10.1016/S0076-6879(09)64009-X).
- Patil, H., Kulkarni, V., Majumdar, S., Repka, M.A., 2014. Continuous manufacturing of solid lipid nanoparticles by hot melt extrusion. *Int. J. Pharm.* <https://doi.org/10.1016/j.ijpharm.2014.05.024>.
- Patil, H., Feng, X., Ye, X., Majumdar, S., Repka, M.A., 2015. Continuous production of Fenofibrate solid lipid nanoparticles by hot-melt extrusion technology: a systematic study based on a quality by design approach. *AAPS J.* <https://doi.org/10.1208/s12248-014-9674-8>.
- Patolla, R.R., Chougule, M., Patel, A.R., Jackson, T., Tata, P.N.V., Singh, M., 2010. Formulation, characterization and pulmonary deposition of nebulized celecoxib encapsulated nanostructured lipid carriers. *J. Control. Release.* <https://doi.org/10.1016/j.jconrel.2010.02.006>.
- Patton, J.S., 1996. Mechanisms of macromolecule absorption by the lungs. *Adv. Drug Deliv. Rev.* [https://doi.org/10.1016/0169-409X\(95\)00113-L](https://doi.org/10.1016/0169-409X(95)00113-L).
- Phan, H.T., Haes, A.J., 2019. What does nanoparticle stability mean? *J. Phys. Chem. C* 123, 16495–16507. <https://doi.org/10.1021/acs.jpcc.9b00913>.
- Pilcer, G., Amighi, K., 2010. Formulation strategy and use of excipients in pulmonary drug delivery. *Int. J. Pharm.* <https://doi.org/10.1016/j.ijpharm.2010.03.017>.
- Puglia, C., Sarpietro, M.G., Bonina, F., Castelli, F., Zammataro, M., Chiechio, S., 2011. Development, characterization, and in vitro and in vivo evaluation of benzocaine- and lidocaine-loaded nanostructured lipid carriers. *J. Pharm. Sci.* <https://doi.org/10.1002/jps.22416>.
- Repka, M.A., Battu, S.K., Upadhye, S.B., Thumma, S., Crowley, M.M., Zhang, F., Martin, C., McGinity, J.W., 2007. Pharmaceutical applications of Hot-Melt Extrusion: Part II. *Drug Dev. Ind. Pharm.* 33, 1043–1057. <https://doi.org/10.1080/03639040701525627>.
- Repka, M.A., Majumdar, S., Battu, S.K., Srirangam, R., Upadhye, S.B., 2008. Applications of hot-melt extrusion for drug delivery. *Expert Opin. Drug Deliv.* <https://doi.org/10.1517/17425240802583421>.
- Rivolta, I., Panariti, A., Lettieri, B., Sesana, S., Gasco, P., Gasco, M.R., Masserini, M., Miserocchi, G., 2011. Cellular uptake of coumarin-6 as a model drug loaded in solid lipid nanoparticles. *J. Physiol. Pharmacol.* 62 (1), 45–53.
- Schuster, B.S., Suk, J.S., Woodworth, G.F., Hanes, J., 2013. Nanoparticle diffusion in respiratory mucus from humans without lung disease. *Biomaterials.* <https://doi.org/10.1016/j.biomaterials.2013.01.064>.
- Shadambikar, G., Kipping, T., Di-Gallo, N., Elia, A.G., Knüttel, A.N., Treffer, D., Repka, M.A., 2020. Vacuum compression molding as a screening tool to investigate carrier suitability for hot-melt extrusion formulations. *Pharmaceutics.* <https://doi.org/10.3390/pharmaceutics12111019>.
- Shadambikar, G., Marathe, S., Patil, A., Joshi, R., Bandari, S., Majumdar, S., Repka, M., 2021. Novel Application of Hot Melt Extrusion Technology for Preparation and Evaluation of Valacyclovir Hydrochloride Ocular Inserts. *AAPS PharmSciTech* 22, 1–7. <https://doi.org/10.1208/s12249-020-01916-5>.
- Shegokar, R., Singh, K.K., Müller, R.H., 2011. Production & stability of stavudine solid lipid nanoparticles - from lab to industrial scale. *Int. J. Pharm.* <https://doi.org/10.1016/j.ijpharm.2010.08.014>.
- Stevens, R.E., Gray, V., Dorantes, A., Gold, L., Pham, L., 2015. Scientific and regulatory standards for assessing product performance using the similarity factor, f2. *AAPS J.* <https://doi.org/10.1208/s12248-015-9723-y>.
- Suk, J.S., Lai, S.K., Wang, Y.Y., Ensign, L.M., Zeitlin, P.L., Boyle, M.P., Hanes, J., 2009. The penetration of fresh undiluted sputum expectorated by cystic fibrosis patients by non-adhesive polymer nanoparticles. *Biomaterials.* <https://doi.org/10.1016/j.biomaterials.2008.12.076>.
- Suk, J.S., Xu, Q., Kim, N., Hanes, J., Ensign, L.M., 2016. PEGylation as a strategy for improving nanoparticle-based drug and gene delivery. *Adv. Drug Deliv. Rev.* <https://doi.org/10.1016/j.addr.2015.09.012>.
- Tiwari, R.V., Patil, H., Repka, M.A., 2016. Contribution of hot-melt extrusion technology to advance drug delivery in the 21st century. *Expert Opin. Drug Deliv.* 13, 451–464. <https://doi.org/10.1517/17425247.2016.1126246>.
- USP Monograph [WWW Document], 2021, URL [http://usp35.infastar.com.cn/uspnf/pub/data/v35300/usp35nf30s0\\_m43724.html](http://usp35.infastar.com.cn/uspnf/pub/data/v35300/usp35nf30s0_m43724.html).
- Yang, W., Peters, J.L., Williams, R.O., 2008. Inhaled nanoparticles-a current review. *Int. J. Pharm.* <https://doi.org/10.1016/j.ijpharm.2008.02.011>.
- Zhang, P., Shadambikar, G., Almutairi, M., Bandari, S., Repka, M.A., 2020. Approaches for developing acyclovir gastro-retentive formulations using hot melt extrusion technology. *J. Drug Deliv. Sci. Technol.* <https://doi.org/10.1016/j.jddst.2020.102002>.